JOURNAL OF MATERIALS SCIENCE **38** (2003) 3945–3953

Liquid phase processing and thin film deposition of titania nanocrystallites for photocatalytic applications on thermally sensitive substrates

M. LANGLET*, A. KIM, M. AUDIER
Laboratoire des Matériaux et de Génie Physique, UMR CNRS 5628, ENSPG-INPG, BP 46, Domaine Universitaire, 38402 Saint Martin d'Hères, France
E-mail: Michel.Langlet@inpg.fr

C. GUILLARD, J. M. HERRMANN
Laboratoire de Photocatalyse, Catalyse et Environnement, IFOS, UMR CNRS 5621, Ecole Centrale de Lyon, BP 163, 69131 Ecully-Cedex, France

Titania films were deposited from sols peptized in acidic conditions and subsequently autoclaved. The microstructural, morphological, optical, and photocatalytic properties of titania films were studied with respect to sol-gel processing parameters. It is shown that films deposited at room temperature are well-crystallized and exhibit good optical quality. Their photocatalytic activity was verified through malic acid decomposition tests. From comparisons with a previous work, processing the sol in acidic conditions is found to be more advantageous than in basic conditions. Using this low temperature approach, titania films could be deposited on thermally sensitive polymer substrates for new photocatalytic applications.

1. Introduction

The sol-gel process is a wet chemistry versatile method based on the hydrolysis/polycondensation of metal alkoxide precursors, which leads to a large variety of oxide materials with multiple properties. Since pioneering studies performed on sol-gel derived photocatalysts in the early 90's [for instance see ref. 1], sol-gel processing of photocatalytic TiO_2 films has been the subject of a growing interest. Under UV-irradiation with photon energy equal to or greater than TiO_2 band gap (for anatase: $h\nu > 3.2$ eV, i.e., $\lambda < 380$ nm), photocatalytic titania films yield the oxidative decomposition of organic matter [2–4]. Thus, sol-gel deposited TiO_2 films have been studied for self-cleaning, depollution, deodorizing, and anti-fouling applications [5–10]. However, good photocatalytic activities of such films necessitate (i) an efficient photo-induced electron-hole pair generation, and (ii) an efficient charge separation, which requires in turn preparations of well crystallized titania films, preferably in the anatase polymorphic form [2]. Since crystallization of amorphous sol-gel TiO_2 films requires a post-deposition thermal treatment at relatively high temperature, photocatalytic applications were essentially restrained to supports of high thermal stability, such as fused silica or mineral glasses.

To exploit photocatalytic properties of sol-gel derived titania films deposited on thermally sensitive substrates, such as polymer supports, a crystallization occurring at low temperature is required. An attractive way to produce photocatalytic films at low temperature relies on the possibility to prepare liquid suspensions of crystallized TiO_2 particles to be deposited using traditional liquid phase deposition techniques, such as spin- or dip-coating. Several works have been devoted to sol-gel preparations of TiO_2 crystallites either in acidic [11–14] or in basic [15, 16] aqueous solutions. In this case, a peptization mechanism is promoted by electrostatic repulsion between either protonated (acidic peptization) or deprotonated (basic peptization) hydrolyzed species, which counteracts the particle agglomeration induced by natural attractive Van der Waals forces and reduces the polycondensation rate. The sols were then refluxed [11, 12, 14–16] or autoclaved [13, 15, 16] for several hours or days in a temperature range of [80–250°C], which led to TiO_2 crystallite formation. Most of these studies have been devoted to ceramic applications, where the crystalline powder was recovered by centrifugation after thermal treatment of the sol, or restricted to fundamental studies of the crystallite structures and crystallization mechanisms. To our knowledge, photocatalytic properties of those powders have rarely been studied and no work reports on sol-gel preparation of stable suspensions compatible with the deposition of optical quality photocatalytic TiO_2 films.

In a previous work, we have proposed a new sol-gel approach based on a liquid phase processing of solutions compatible with a room temperature deposition of photocatalytic TiO_2 films on polymer substrates

*Author to whom all correspondence should be addressed.

[17]. Nanocrystalline films of rather good optical transparency could be produced. TiO_2 nanocrystallites were formed in basic aqueous solution, which was either refluxed or autoclaved. We showed that better results could be obtained after autoclaving. The film photoactivity appeared to be similar to this of sol-gel films crystallized at high temperature. However, this liquid solution approach suffered from some limitations since the film optical quality remained partly affected by the presence of micro-particles related to a sol processing in basic conditions. The amount of micro-particles could only be reduced by lowering the TiO_2 precursor concentration in the sol, which imposed a long multi-layer deposition procedure to obtain films of consequent thickness. Besides, the preparation of an aqueous sol was not compatible with a deposition of homogeneous films, due to the high surface tension of water that promoted de-wetting effects. Thus, a reconcentration/exchange procedure was performed after the sol heat-treatment. The reconcentration step aimed at increasing the final TiO_2 concentration, in order to reduce the multi-layer procedure duration, and the exchange step was performed with ethanol, to take advantage of the low surface tension of this solvent. The aqueous sol was first thermally reconcentrated 10 times to evaporate the major part of water. It was then diluted with 66 volume fractions of absolute ethanol and subsequently thermally reconcentrated 67 times. During this last step, most of the remaining water was evaporated in the form of a water-ethanol azeotrope. This yielded a quite long overall sol processing.

In this paper, we describe the sol-gel processing of TiO_2 crystallite suspensions from sols prepared in acidic conditions and subsequently autoclaved. Thin films were deposited at room temperature from the resulting sols. The experimental conditions are described and discussed with respect to morphological, microstructural, optical, and photocatalytic properties of the films. With respect to films deposited from basic sols, the present method is shown to be much more flexible and efficient for photocatalytic applications on thermally sensitive substrates.

2. Experimental

A mother solution was prepared from TIPT (tetraisopropyl orthotitanate from Fluka) diluted in absolute ethanol and peptized in acidic conditions. The TIPT concentration was fixed at 0.40 M. Various amounts of hydrochloric acid were used to study the effect of pH in the final aqueous sol. This mother solution was then added dropwise at room temperature into a given volume of water under magnetic stirring. Such partial redilution in water caused slight increases in the solution pH and correspondingly slight decreases in TIPT concentration. Compositions of aqueous sols tested in this study are summarized in Table I: pH, TIPT concentration (C_{TIPT}) and water to TIPT molar ratio (r_w) in aqueous sols were varied in ranges of [1.27–2.00], [0.24–0.40 M] and [0.8–90], respectively. Compared to a previous approach, for which a high r_w value of 1860 was used [17], we tested here very low r_w values in order to simplify the subsequent exchange procedure with ethanol. Sols were then heat-treated for 6 h in a stainless steel autoclave placed in a tubular furnace. Autoclaving temperatures from 100°C up to 200°C were studied. Thermal regulation was achieved using a thermocouple inserted in the wall of the autoclave. After thermal treatment, an exchange procedure with ethanol was performed in order to remove water. Sols were first thermally reconcentrated 10 times and then diluted 10 times in ethanol. Compared to a previous work, this procedure was, therefore, much shorter. A complementary reconcentration was also tested in order to prepare sols with greater C_{TIPT}. Sols were finally ultrasonicated for various times between 1 and 6 h. The overall protocol is summarized in Fig. 1. More detailed conditions are presented as part of the results.

TABLE I Water to TIPT molar ratio, pH, and TIPT concentration, for solutions peptized in acidic conditions. Experimental data correspond to the composition of the autoclaved aqueous sol. The pH value was calculated from the hydrochloric acid amount. For solutions A1, A2, A3, and A6, pH variations correspond to dilutions effects induced by mixing the mother solution with water. For solutions A4 and A5, the pH was adjusted by varying the amount of hydrochloric acid in the mother solution. Solution A7 was prepared in the same conditions as solution A6 and additionally reconcentrated twice after the exchange procedure

Solution	r_w	pH	C_{TIPT}
A1	0.8	1.27	0.40 M
A2	15	1.31	0.36 M
A3	30	1.35	0.33 M
A4	30	1.60	0.33 M
A5	30	2.00	0.33 M
A6	90	1.48	0.24 M
A7	90	1.48	0.24 ≥ 0.48 M

Thin films were deposited by spin-coating at room temperature. Liquid volumes between 2 and 6 μl were radially spread with rotating speeds between 2500 and 6000 rpm, depending on the substrate nature and sol viscosity. Film depositions were performed on (100) silicon wafers for routine characterizations and on polycarbonate (PC) substrates for punctual UV/visible transmission and photocatalytic activity measurements. Films of different thicknesses were deposited using a

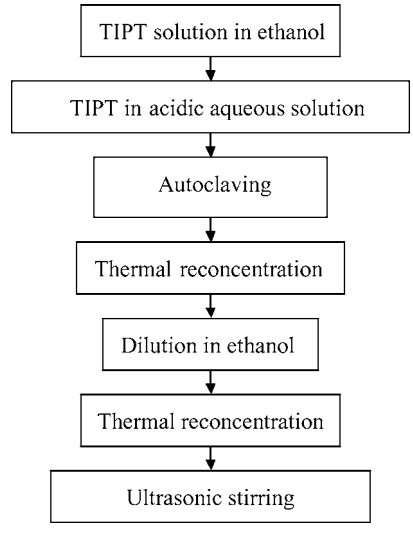

Figure 1 Overall protocol used for the processing of acidic TiO_2 sols.

multi-layer deposition procedure, i.e., each single-layer was heat-treated at 100°C for about 30 s before deposition of another layer. Such heat-treatment was necessary to remove a rest of water still present in the sol after the exchange procedure. When water was not correctly eliminated, cracks appeared in the film during the multi-layer deposition procedure.

The sol viscosity was measured using a rotating cylinder viscosimeter (Rheovisco ELV-8). Fourier transform infrared (FTIR) transmission spectra of films deposited on silicon were recorded in a [4000–250 cm^{-1}] range with a resolution of 4 cm^{-1} using a Bio-Rad FTS-165 spectrometer. Spectra of 300 scans were measured at room temperature. They were analyzed after subtracting the bare Si substrate spectrum. For transmission electron microscope (TEM) investigations, small fragments obtained by scraping thin film samples were deposited on copper grids coated with a carbon film. A JEOL 200CX microscope was used in a configuration allowing large tilt angles of the specimen (±45°) and a lattice fringe resolution of 3.2 Å. A Philips XL 30 scanning electron microscope (SEM) was used to study film surface morphologies. The surface quality of films was also investigated from optical microscopy (Leica DMLM) in dark field mode. Thickness and refractive index of films deposited on silicon were measured using a Sentech ellipsometer at 632 nm wavelength. Visible transmittance spectra of films deposited on PC were measured in a [200–1100 nm] range using a Jasco V-530 spectrophotometer.

The photocatalytic activity was measured at room temperature. Titania films deposited on Si or PC were settled in a photoreactor containing malic (2-hydroxybutanedioic) acid aqueous solution (3.7×10^{-4} mol/l) and exposed to UV-irradiation provided by a Philips HPK 125 UV-lamp using a Corning 0.52 filter ($\lambda > 340$ nm). Small solution aliquots were periodically withdrawn in order to measure the concentration variations of malic acid as a function of time. Malic acid analysis was performed by liquid chromatography (HPLC) using a "Waters 600" chromatograph, equipped with a SARASEP CAR-H column (eluent: H_2SO_4, 5×10^{-2} M; flow rate: 0.7 ml/min; detection at $\lambda = 210$ nm). The photocatalytic activity was identified as the rate of disappearance of malic acid. This acid has been chosen as a model molecule of carboxylic acids, which are the best representatives for the main constituents of intermediate products in oxidative degradation processes [2].

3. Results and discussion

3.1. Acidic sol preparation

When mixing the ethanolic mother solution in water, we observed that gelation occurred rapidly when the initial solution was not preliminarily aged for a sufficient time. Since acidic peptization inhibits the polycondensation reaction, chemically stable sols should be obtained. However, it is known that the peptization process is thermally activated and its rate drops dramatically below 80°C [14]. For this reason, a sufficient aging time at room temperature was necessary to protonate the titanium species and to achieve an efficient peptization. Thus, the solution was aged for 60 h at room temperature before being mixed with water. We also observed that precipitation occurred rapidly during mixing with water when the initial solution did not already contain a small amount water. Conversely, when a small quantity of water was preliminarily diluted in the initial solution, no precipitation occurred. In a previous work, we showed that optimal stabilization effects could be obtained using a solution with $C_{TIPT} = 0.40$ M, pH = 1.27 and $r_w = 0.8$ [18]. This solution was finally used as mother solution. The stability of the derived aqueous sols was promoted by acidic peptization effects. The hydrolysis reaction proceeds rapidly in the presence of a large excess of water. In acidic conditions, protonation of hydrolyzed species occurs all the more easily as less acidic species are formed, i.e., when the Ti–O–Ti species are few condensed. Consequently, acidic conditions favor a stabilization of weakly cross-linked species and the particle growth is inhibited by peptization in the early stage of polycondensation. Let us note that basic conditions promote a reverse trend. Since basic peptization occurs all the more easily as more acidic, and thus more polycondensed, species are formed, basic conditions biase the sol-gel transformation toward particle growths. For instance, it is known that three-dimensional silica particles are formed via the sol-gel route in basic conditions, while in acidic conditions linear Si–O–Si chains tend to be formed [19]. The three-dimensional particle formation is all the more marked in the case of titanium solutions. Owing to a strong sol-gel reactivity of titanium alkoxides in nearly neutral pH conditions, dense three-dimensional particles are obtained for pH exceeding a value of 3, while short Ti–O–Ti chains are obtained for pH lower than 2 [18, 20]. Accordingly, aqueous sols prepared with pH between 1.27 and 2.0 remained transparent and stable for the whole r_w range studied here (Table I). Only a slight increase in viscosity was measured after mixing with water, which was probably due to a limited sol-gel reaction. These good stabilization features allowed us to process sols with high TIPT concentrations (0.23 to 0.4 M). Conversely, larger particles induced by basic peptization conditions tended to sediment rapidly, which imposed to process very weakly concentrated sols (2.8×10^{-2} M) [17].

3.2. Sol processing

Aqueous sols were autoclaved at temperatures between 100 and 200°C. After autoclaving, the sol with $r_w = 0.8$ appeared to be transparent, while thick pastes were observed to form and to sediment for the other sols (Table I). These pastes could easily be redispersed through ultrasonication or magnetic stirring for a few tens of minutes. The sol was then exchanged with ethanol. After exchange, the sol with $r_w = 0.8$ remained transparent and stable. All the other sols became milky and tended again to sediment rapidly. A new ultrasonic treatment was necessary to minimize sedimentation. Sedimentation features and milky appearance of sols arise from aggregation of oxide particles, which are partially linked together by some remnant Ti–O–Ti chains promoted by the acidic conditions. These chains

are likely broken though ultrasonication. After deagglomeration, oxide particles are stabilized in the solution by acidic peptization effects. Such effects will be discussed below with respect to the optical quality of films. Ultrasonication was performed for 1 to 6 h, depending on the sol processing conditions. Sols processed at 200°C, with a pH between 1.35 and 1.5 and a $r_w \geq 30$, necessitated shortest ultrasonic stabilization times and exhibited weakest sedimentation effects, while longer ultrasonication times were necessary for other sols. After optimization of the ultrasonication duration, only a very slow sedimentation occurred during subsequent aging of sols at room temperature. This behavior probably arises from a progressive particle reagglomeration resulting from the competition between electrostatic repulsion and natural attractive Van der Waals forces. In any cases, a short magnetic stirring performed before deposition allowed us to obtain films of good optical transparency. The sol viscosity was observed to depend closely on experimental conditions: it increased with r_w and C_{TIPT}. For instance, a viscosity of 6 cP was measured for a sol autoclaved at 200°C with $r_w = 30$ and $C_{TIPT} = 0.33$ M. Values up to 10 cP were measured for higher C_{TIPT} or r_w. Thus, the film deposition conditions had to be adjusted with respect to the sol processing conditions. The viscosity also tended to increase with time after sol processing, but aged sols recovered their initial viscosity after magnetic stirring for a few minutes. In such conditions, thin films could be deposited in reproducible conditions over a solution aging period of several months.

3.3. Crystallization features

Fig. 2 shows the FTIR spectra of films issued from sols autoclaved at 100 or 200°C for 6 h with different r_w and pH values. For a sol autoclaved at 100°C, with $r_w = 0.8$ and pH = 1.27, the film spectrum exhibits a broad band centered at around 470 cm^{-1}, with several additional small bands located between 1000 and 500 cm^{-1}. It is the typical spectrum of TiO_2 oxopolymer corresponding to an amorphous TiO_2 network with chain-end alkoxy or hydroxyl groups [21]. This

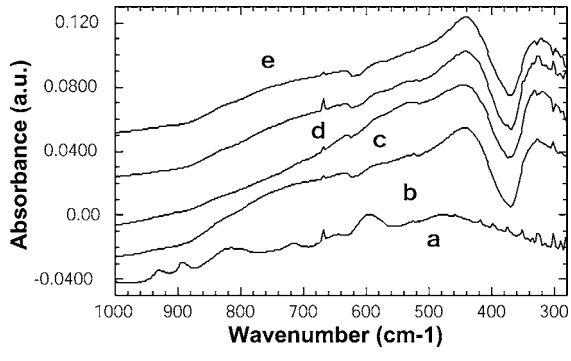

Figure 2 FTIR spectra of films deposited from various sols: (a) sol autoclaved at 100°C with $r_w = 0.8$ and pH = 1.27, (b) sol autoclaved at 200°C with $r_w = 15$ and pH = 1.31, (c) sol autoclaved at 100°C with $r_w = 30$ and pH = 1.35, (d) sol autoclaved at 200°C with $r_w = 30$ and pH = 1.35, and (e) sol autoclaved at 200°C with $r_w = 30$ and pH = 2.00. Small and sharp peaks located around 670 cm^{-1} and below 400 cm^{-1} correspond to atmospheric CO_2 and H_2O, respectively.

spectrum indicates that crystallization does not occur by autoclaving for a r_w value as low as 0.8. For $r_w \geq 15$, all the spectra exhibit two bands at around 440 and 330 cm^{-1}, which correspond to transverse optical (TO) vibration modes of anatase [22]. In our previous study, we showed that band intensities and shapes are closely related to film crystallization degrees and crystallite sizes [17]. For amorphous films, both bands overlap and constitute a single broad band around 400 cm^{-1}. As crystallization takes place, they increase in intensity and sharpen, thus forming two separate bands. Well-resolved bands observed in Fig. 2 indicate that for $r_w \geq 15$, crystallization takes place in a large extent after 6 h autoclaving, in the whole range of pH (between 1.3 and 2.0) and autoclaving temperatures (between 100 and 200°C) tested here. Let us note that for crystalline films, traces of water but no alkoxy groups could be detected by FTIR.

Fig. 3 shows a selected area electron diffraction (SAED) pattern and corresponding bright and dark field TEM images, as well as a high resolution TEM image, for a film deposited from a sol autoclaved at 200°C with $r_w = 30$. These TEM images show that crystallite sizes are less than 10 nm. Rings of reflections observed on the corresponding SAED pattern are characteristic of a well crystallized anatase phase, i.e., ring positions and intensities are in good agreement with a calculated pattern from crystallographic data [23] and electron scattering amplitudes of Ti and O elements [24]. In some cases, a diffraction ring was also observed at about 2.2 $Å^{-1}$, which corresponded to traces of brookite. In agreement with FTIR experiments, additional TEM analysis showed that anatase nanocrystallites were produced in the whole range of experimental conditions tested here, provided that the sol was prepared with $r_w \geq 15$.

During the sol-gel transformation of titanium alkoxides, hydrolysis and polycondensation usually take place simultaneously. The so-formed oxide species are thus affected by non-hydrolyzed alkoxy groups, which act as structural impurities in the oxide network and inhibit the particle crystallization. Amorphous $TiO_x(OH)_y(OR)_z$ particles (where R is an alkyl radical) are formed in this case. To promote crystallization, it is therefore important that hydrolysis goes to completion before polycondensation proceeds significantly. In other words, a good balance between hydrolysis and polycondensation reaction kinetics is required. FTIR and TEM studies show that this requirement was reached from acidic sols prepared with $r_w \geq 15$. Above this water amount threshold, hydrolysis is favored by acidic catalysis conditions via a nucleophilic attack mechanism. On the other hand, polycondensation is partly inhibited through acidic peptization effects, i.e., by electrostatic repulsion between protonated hydrolyzed species [11, 14]. In such conditions, alkoxy-free $TiO_x(OH)_y$ hydroxyl species are formed. During autoclaving, these species polycondense and cross-link to form pure oxide clusters, which act as nucleation centers for a subsequent growth of TiO_2 anatase crystals [11–16]. Thus, the formation of pure oxide nucleation sites depends on a sufficient amount of water and on an efficient peptization process, which is controlled

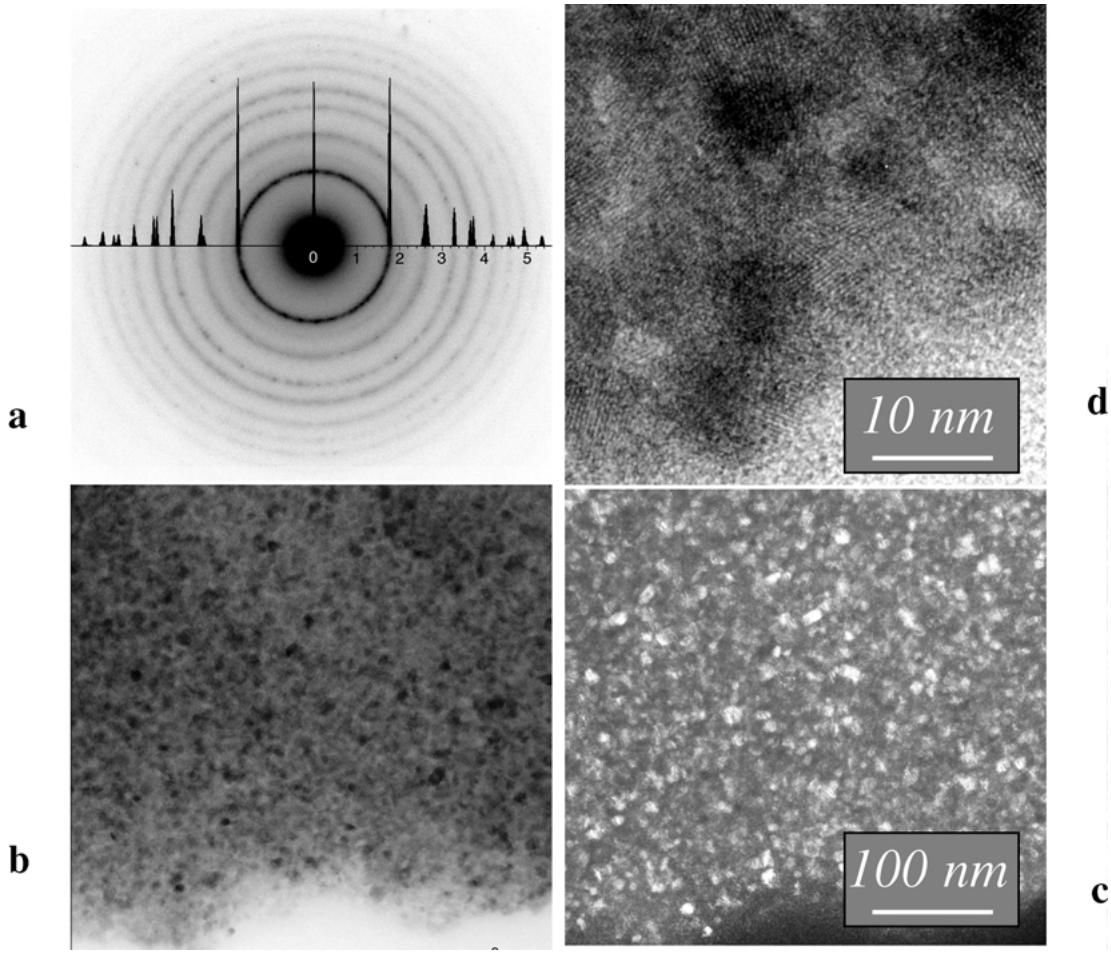

Figure 3 SAED pattern (a) with corresponding bright (b) and dark field (c) TEM images, and high resolution TEM image (d), for a film deposited from a sol autoclaved at 200°C with $r_w = 30$. The dark field image was obtained by selecting part of the first electron diffraction ring. Reflections are identified on the SAED pattern by comparing with a simulation of the anatase diffraction pattern. Diffraction peak positions are given in Q units ($Å^{-1}$).

by the pH. Both reactions are also thermally activated. However, from FTIR and TEM results it appears that, above a r_w threshold of about 15, both the role of pH (between 1.3 and 2.0) and autoclaving temperature (between 100 and 200°C) become minor because polycondensation is sufficiently inhibited and hydrolysis sufficiently catalyzed. These results are in agreement with those of Bischoff *et al.* who mentioned that, in the presence of a large excess of water, crystallization of sol-gel TiO_2 particles was governed by kinetics rather than by thermodynamics [14]. Wang *et al.* have also reported that autoclaving conditions do not influence noticeably the size and crystallization degree of sol-gel derived anatase particles, provided that thermal treatment be performed with a sufficient amount of water [25]. For acidic peptization conditions, our results confirm that, in the thermal [100–200°C] range and above a r_w value around 15, crystallization would be a kinetic process promoted by balanced hydrolysis/polycondensation kinetics.

3.4. Optical quality and morphology of the films

Fig. 4 shows UV/visible transmission spectra and optical microscopy dark field images for multi-layer films of various thickness deposited on polycarbonate substrates. The sol was autoclaved at 200°C with various r_w (sols A2, A3, and A6 in Table I), and finally ultrasonicated for 1 h. For the sol prepared with $r_w = 15$, light transmission was observed to continuously decrease with increasing thickness, which depicts significant optical losses (Fig. 4a). The corresponding optical microscope image of Fig. 4a shows the presence of numerous large particles at the film surface, with a wide size distribution (a few tenths to several tens of micrometers), which explains the poor optical quality of this film. For a sol with $r_w = 30$ (Fig. 4b), the spectra exhibit pronounced interference effects, which are due to multi-reflections at the film-air and film-substrate interfaces. For a transparent film of high refractive index deposited on a transparent substrate of lower refractive index, transmission maxima are obtained when the film optical thickness corresponds to even multiples of the quarter-wavelength. At these wavelengths, the film is theoretically optically non-active, i.e., for an optical quality film, the transmission values should fit the bare substrate transmission. Transmission minima are obtained when the film optical thickness corresponds to odd multiples of the quarter-wavelength, i.e., when the mismatch of refractive indices between substrate and film induces a maximum of reflection. In Fig. 4b, the transmission maxima observed in a [500–1100 nm] spectral range appear to fit closely the transmission

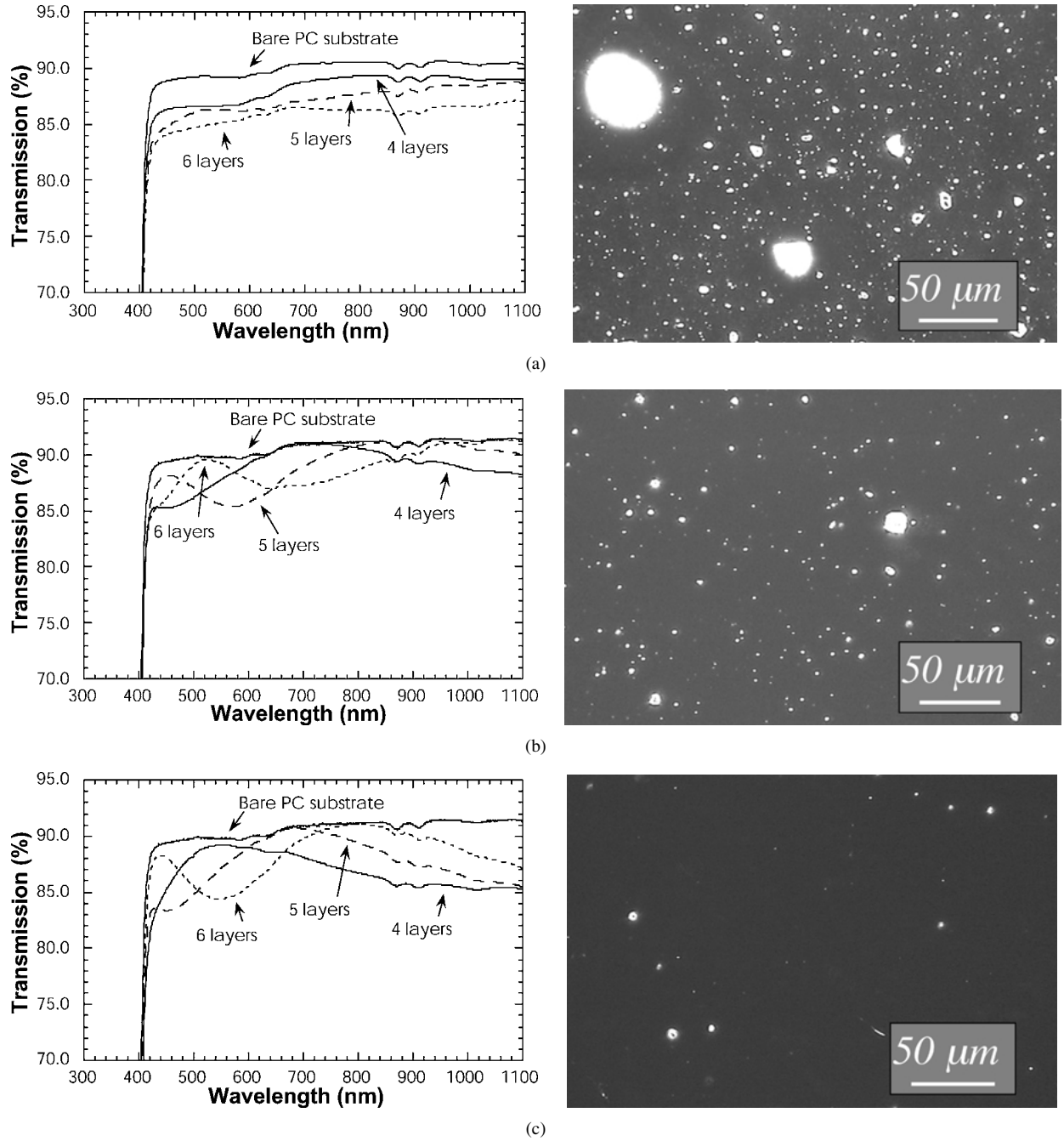

Figure 4 UV/visible transmission spectra and optical microscope dark field images for multi-layer films of various thickness issued from sols autoclaved at 200°C with: (a) $r_w = 15$, (b) $r_w = 30$, and (c) $r_w = 90$. For transmission measurements, the films were deposited on PC, and their spectra are compared with that of a bare PC substrate.

level measured for the bare substrate. Optical losses in the visible range are therefore negligible. In a [400–500 nm] range, the transmission losses remain weak (about 1%). No transmission could be measured below 400 nm, because of the PC substrate absorption. The corresponding image of Fig. 4b shows that the amount of large particles is considerably reduced, compared to the image of Fig. 4a. In particular, largest particles of several tens of micrometers have completely disappeared. SEM observations of this film (not illustrated here) depicted a homogeneous granular surface with a grain size of about 100 nm. Such grains correspond to aggregates of nanocrystallites. Aggregates presumably result from a competition between electrostatic repulsion and Van der Waals forces within the sol. Similar aggregates were observed for all the films deposited from sols autoclaved with $r_w \geq 15$. Note that for $r_w = 0.8$, the optical transparency appeared very good and any aggregation was not observed, but in that case, no crystallization occured.

The optical transmission is also excellent for films obtained at $r_w = 90$ (Fig. 4c). In this case, the amount of large particles appears even smaller than that depicted in Fig. 4b. A similar optical quality was also obtained from a solution with $r_w = 90$ reconcentrated twice (final C_{TIPT} of 0.48 M instead of 0.24 M, sol A7 in Table I). In summary, only 1 h ultrasonication yielded very good optical films for sols autoclaved at 200°C with $r_w \geq 30$ and a pH between 1.35 and 1.5. Let us recall that the film optical quality could be reproduced using the same solution over a period of several months. For lower r_w and temperature or greater pH, the

optical quality was less good after 1 hour ultrasonication. This was related to a greater amount of large grains at the film surface. However, a good optical quality was again obtained when increasing the ultrasonication duration up to 6 h. This behavior agrees fairly well with aforementioned sedimentation features. The presence of large grains at the film surface is directly related to the sol processing conditions. Since in acidic solution, crystallization competes with the development of Ti—O—Ti chains, these chains tend to link the crystallites and favor the formation of aggregates, which undergo sedimentation and affect the film optical quality. In adequate hydrolysis/peptization conditions, this competitive mechanism is biased toward crystallization, which reduces the agglomerate formation. Besides, Ti—O—Ti chains can readily be broken after a short ultrasonic treatment and crystallites are rapidly de-agglomerated. Conversely, for lower r_w and temperatures, as well as for greater pH, the sol-gel reaction in autoclave is biased toward chain formation, which promotes greater crystallite bonding. Consequently, a longer ultrasonic treatment is necessary. Note that in basic conditions, large three-dimensional particles could not be broken by ultrasonication. Therefore, acidic conditions yielded a significant improvement compared to films derived from basic sols, for which, in optimized conditions, the optical losses were 1–2% in the visible range and increased up to 5% below 500 nm [17].

3.5. Film thickness and porosity

The good optical quality of films deposited from acidic sols allowed us to reliably measure their thickness and refractive index by ellipsometry. Fig. 5 shows the film thickness and refractive index variations versus the number of single-layers, for multi-layer films deposited from sols autoclaved at 130°C with $r_w = 30$ or 90 (sols A3 and A6). The film thickness monotonically increases with the number of single-layers, which demonstrates a good control of the deposition conditions. Fig. 5 also depicts a slight increase of the refractive index, which suggests that the film density increases with the number of single-layers. It might be possible that, after each single layer deposition, part of the liquid penetrates inter-granular pores of the previously deposited layer, allowing smallest crystallites to fill in the pores. Fig. 5 also shows that films deposited from a sol with $r_w = 90$ exhibit a greater refractive index ($n = 1.96 \pm 0.06$, depending on film thickness) than films deposited from a sol with $r_w = 30$ ($n = 1.87 \pm 0.07$). Such an effect of r_w was also observed for sols autoclaved at 200°C (Table II). In addition, Table II shows that films deposited from sols autoclaved at higher temperature exhibit weaker refractive index. For instance, a refractive index of 1.70 ± 0.04 or 1.85 ± 0.05 was measured for films deposited from a sol autoclaved at 200°C with $r_w = 30$ or 90, respectively. Reasons for such features have not been elucidated yet. According to FTIR and TEM results, we can assume that nearly pure TiO_2 films were deposited. In that case, the film porosity can be fairly well estimated from the refractive index value, using the Lorentz-Lorentz relationship [26] and the bulk anatase refractive index ($n \approx 2.50$) [27]. For the aforementioned films, the porosity was estimated to range between about 25 and 40 vol%, depending on film thickness and sol processing conditions (Table II).

TABLE II Refractive index and porosity of films deposited from sols autoclaved at 130 or 200°C with $r_w = 30$ or 90. The refractive index corresponds to the average value calculated from films with various thickness (see text). The film porosity was estimated from the refractive index value, using the Lorentz-Lorentz relationship

r_w	T (°C)	n (632 nm)	P (vol%)
30	130	1.87 ± 0.07	29 ± 4
30	200	1.70 ± 0.04	39 ± 3
90	130	1.96 ± 0.06	24 ± 4
90	200	1.85 ± 0.05	30 ± 3

3.6. Photocatalytic properties

Our results indicate the possibility to deposit crystalline films at room temperature. Consequently, such films could be deposited on PC substrates. The photoinduced decomposition of malic acid was studied for films of similar thickness (about 200 nm) deposited on PC and silicon from a sol autoclaved at 200°C with $r_w = 30$ (Fig. 6). It appears that about 18 mol% of malic acid is decomposed after 2 h UV-irradiation for the film deposited on silicon. For the film on PC, the photocatalytic activity is about 25% weaker. Such an influence of the substrate was previously observed for

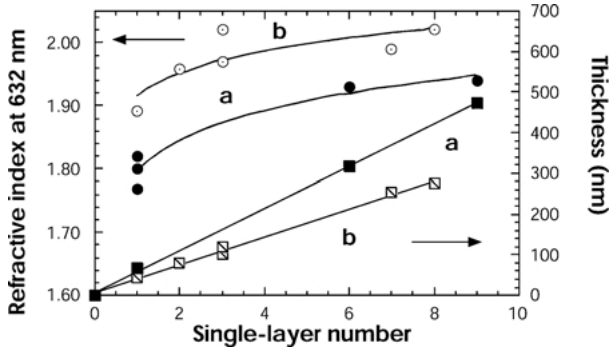

Figure 5 Thickness and refractive index versus single-layer number for multi-layer films deposited from sols autoclaved at 130°C with (a) $r_w = 30$, and (b) $r_w = 90$.

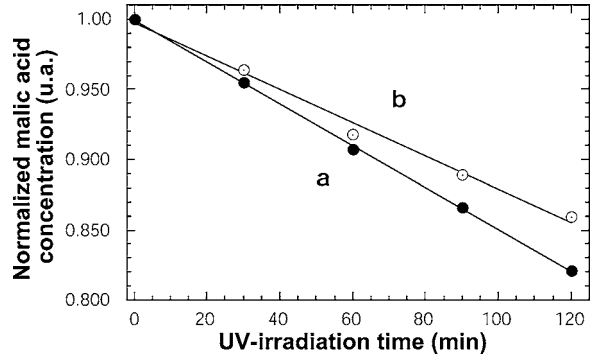

Figure 6 Malic acid photocatalytic decomposition curves for 200 nm thick films deposited on (a) silicon, and (b) PC substrate.

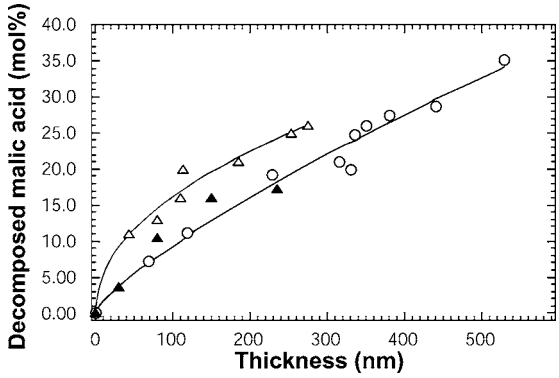

Figure 7 Concentration of decomposed malic acid after 2 h UV-irradiation versus film thickness. The films were deposited at room temperature on Si from a sol autoclaved at 200°C with $r_w = 30$ (o), and on Si (Δ) or PC (▲) from a sol autoclaved at 130°C with $r_w = 90$.

films deposited from basic sols [17]. It was attributed to multi-reflections of the UV radiation occurring within films deposited on silicon, which favored the creation of additional photo-induced electrons and holes. In the present work, the lower activity observed on PC could not be correlated with any sample degradation. In particular, no photocatalytic decomposition of the organic support could be evidenced. It is therefore assumed that, here again, the greater photoactivity on silicon was due to optical effects. Fig. 7 shows the thickness dependence of the photocatalytic activity for films deposited on silicon and PC from sols autoclaved at 130°C ($r_w = 90$) or 200°C ($r_w = 30$). Fig. 7 confirms that the photoactivity of films deposited on PC is about 25% weaker than that measured for films on silicon. From Fig. 7, it also appears that the photocatalytic activity continuously increases with the film thickness, meaning that the inner part of films participates to malic acid photodecomposition. This observation implies that stronger catalytic activities can be reached for thicker films. However, Fig. 7 shows that this photoactivity increases more slowly than film thickness. For a true heterogeneous catalytic regime, the reaction rate is directly proportional to the mass of catalyst [2], i.e., the photoactivity should increase linearly with film thickness. In addition, films deposited from the sol autoclaved at 130°C with $r_w = 90$ exhibited a stronger photoactivity than films deposited from the sol autoclaved at 200°C with $r_w = 30$. Since crystallization degrees, which determine the photo-induced charge carrier generation in TiO_2 grains, are similar for both sols, it is concluded that differences illustrated in Fig. 7 are induced by another factor. Let us recall that the volume porosity was deduced to be around 25 and 40% for films deposited from the sol autoclaved at 130°C with $r_w = 90$ and the sol autoclaved at 200°C with $r_w = 30$, respectively. The film porosity is another factor that could account for thickness effects illustrated in Fig. 7. For a same thickness, denser films are richer in TiO_2 particles than porous ones, which would explain in part the stronger photocatalytic activity of films deposited from the sol autoclaved at 130°C with $r_w = 90$. Besides, liquid or gaseous reactants adsorbed at the film surface might be able to diffuse through the pores, inducing a greater quantity of TiO_2 particles involved in the photocatalytic reaction. In that case, the reactant diffusion should be favored by a greater porosity and, for a same thickness, the photoactivity of more porous films should be stronger than that of dense films. This assumption is denied by variations illustrated in Fig. 7. On the other hand, TiO_2 particles that are not directly in contact with the matter to be photocatalytically decomposed might be able to participate in the photocatalytic process, provided that an efficient transfer of charge carriers occurs between particles [9]. A too high porosity could reduce the intergranular transfer, thus limiting the photocatalytic activity of the film, which seems to be illustrated in Fig. 7. The thickness dependence of photoactivity might therefore be governed by an intergranular transfer. In this case, the recombination of photoinduced electron-hole pairs, occurring during migration from the deeper layers toward the surface in contact with matter to be decomposed, could in turn affect the photocatalytic activity. Such a recombination is known to severely limit the efficiency of photocatalytic reactions [2, 28]. An increase of the recombination probability might explain the non-linear increase of photoactivity with increasing film thickness. The photoactivity of densest films deposited at room temperature on silicon from acidic sols ($T = 130$°C, $r_w = 90$) appeared to be very close to this measured for sol-gel TiO_2 films crystallized at high temperature [17, 29]. It can therefore be concluded that the crystallization degree obtained through liquid phase sol-gel processing is comparable to that obtained after a high temperature film treatment.

4. Conclusion

Crystalline TiO_2 films were deposited at room temperature from sol-gel solutions peptized in acidic conditions and subsequently autoclaved. It is shown that, compared to basic sols, acidic sols can be processed more flexibly in a wide range of experimental conditions compatible with a deposition of crystalline films of good optical quality. The formation of TiO_2 crystallites depends on balanced hydrolysis/polycondensation reaction kinetics, which requires in turn a sufficient amount of water and suitable acidic pH. For $r_w \geq 15$, crystallization was achieved in a pH range of [1.3–2.0], for autoclaving temperatures between 100 and 200°C. On the other hand, greater r_w and temperature values and smaller pH values were observed to favor the deposition of optical quality films. Good crystallization degrees achieved from acidic sols promoted in turn the deposition at room temperature of films with a high photocatalytic efficiency. Consequently, this study opens the field to new applications involving the deposition of photocatalytic films on thermally sensitive materials, such as polymers [30].

Acknowledgements

This work has received financial support from the Philips Lighting Company (Miribel, France) and the French Rhône-Alpes region. The authors thank Mrs M.N. Mozzanega for her contribution to photocatalytic tests.

References

1. S. TUNESI and M. ANDERSON, *J. Phys. Chem.* **95** (1991) 3399.
2. J. M. HERRMANN, *Catalysis Today* **53** (1999) 115.
3. M. R. HOFFMANN, S. T. MARTIN, W. CHOI and D. W. BAHNEMANN, *Chem. Rev.* **95** (1995) 69.
4. N. SERPONE and E. PELIZETTI (eds.), in "Photocatalysis, Fundamentals and Applications" (John Wiley & Sons, New York, 1989).
5. V. ROMEAS, P. PICHAT, C. GUILLARD, T. CHOPIN and C. LEHAUT, *Ind. Eng. Chem. Res.* **38** (1999) 3878.
6. Y. PAZ, Z. LUO, L. RABENBERG and A. HELLER, *J. Mater. Res.* **10**(11) (1995) 2842.
7. A. FERNANDEZ, G. LASSALETTA, V. M. JIMENEZ, A. JUSTO, A. R. GONZALEZ-ELIPE, J.M. HERRMANN, H. TAHIRI and Y. AIT-ICHOU, *Appl. Catal. B: Environ.* **7** (1995) 49.
8. N. NEGISHI and K. TAKEUCHI, *J. Sol-Gel Sci. Tech.* **22** (2001) 23.
9. A. HATTORI and H. TADA, *ibid.* **22** (2001) 47.
10. N. SMIRNOVA, A. EREMENKO, O. RUSINA, W. HOPP and L. SPANHEL, *J. Sol-Gel Sci. Tech.* **22** (2001) 109.
11. K.-N. P. KUMAR, K. KEIZER, A. J. BURGRAAF, T. OKUBO, H. NAGAMOTO and S. MOROOKA, *Nature* **358** (1992) 48.
12. K.-N. P. KUMAR, J. KUMAR and K. KEIZER, *J. Amer. Ceram. Soc.* **77**(5) (1994) 1396.
13. R. R. BACSA and M. GRÄTZEL, *ibid.* **79**(8) (1996) 2185.
14. B. L. BISCHOFF and M. A. ANDERSON, *Chem. Mater.* **7** (1995) 1772.
15. Y. OGURI, R. E. RIMAN and H. K. BOWEN, *J. Mater. Sci.* **23** (1988) 2897.
16. A. CHEMSEDDINE and T. MORITZ, *Eur. J. Inorg. Chem.* **235** (1999).
17. M. LANGLET, A. KIM, M. AUDIER, C. GUILLARD and J. M. HERRMANN, *Thin Solid Films*, in press (2002).
18. M. BURGOS and M. LANGLET, *J. Sol-Gel Sci. Tech.* **16** (1999) 267.
19. C. J. BRINKER and G. W. SCHERER, "Sol-Gel Science, The Physics and Chemistry of Sol-Gel Processing" (Academic Press, San Diego, 1990) p. 194.
20. M. KALLALA, C. SANCHEZ and B. CABANE, *J. Non-Cryst. Sol.* **147/148** (1992) 189.
21. M. BURGOS and M. LANGLET, *Thin Solid Films* **349** (1999) 19.
22. R. J. GONZALES, R. ZALLEN and H. BERGER, *Phys. Rev.* B **55**(11) (1997) 7014.
23. R. W. G. WYCKOFF, "Crystal Structures," Vol. 1 (Interscience Publishers, Inc., New York, 1948) p. 253.
24. "Int. Tables for X-Ray Cryst," Vol. 3 (Lynoch, Birmingham, 1962) p. 217.
25. C. C. WANG and J. Y. YING, *Chem. Mater.* **11** (1999) 3113.
26. M. BORN and E. WOLF, "Principle of Optics" (Pergamon, New York, 1975) p. 87.
27. "Handbook of Chemistry and Physics," 48th ed. (The Chemical Rubber Co., Cleveland (Ohio), 1967) B-279.
28. A. HATTORI, Y. TOKIHISA, H. TADA, N. TOHGE, S. ITO, K. HONGO, R. SHIRATSUCHI and G. NOGAMI, *J. Sol-Gel Sci. Tech.* **22** (2001) 53.
29. M. LANGLET, A. KIM, M. AUDIER and J. M. HERRMANN, *J. Sol-Gel Sci. Tech.* **25** (2002) 223.
30. M. LANGLET, C. VAUTEY and A. KIM, French Patent FR 02 292351.0 (2002).

Received 12 December 2002
and accepted 7 July 2003